SUPPLEMENTAL MATERIALS

ASCE *Journal of Environmental Engineering*

Modeling PFAS Removal Using Granular Activated Carbon for Full-Scale System Design

Jonathan B. Burkhardt, Nick Burns, Dustin Mobley, Jonathan G. Pressman, Matthew L. Magnuson, and Thomas F. Speth

DOI: 10.1061/(ASCE)EE.1943-7870.0001964

www.ascelibrary.org

Supplemental Methods

Pilot Study

Between August 2017 and August 2018, a 20-MGD utility conducted a two-phase pilot study. The pilot study was conducted in preparation for installing PFAS treatment for a future capacity of 44-MGD system. Raw water was supplied to two pilot columns with GAC and treated water within their treatment train was supplied to an additional nine columns containing GAC or anion exchange resin media. The 2 columns tested with raw water were intended to capture the potential impact of a stopgap measure of replacing this system's biologically activated carbon with fresh GAC, while the deep-bed GAC treatment was being installed. This manuscript evaluates only the GAC piloting data. Pilot columns were 4-in (10 cm) diameter and 4-ft (120 cm) long. The flowrate through the columns was maintained at 0.26 gpm (980 ml min^{-1}) throughout all stages of piloting, which corresponds to a 10-min empty bed contact time (EBCT).

Phase I was conducted for 125 days and included three types of GAC (Calgon F300, Calgon F400, and Evoqua 1230AWC) in four pilot columns (Aug–Dec 2017). Columns containing Calgon F300 and F400 GACs were fed raw water influent to the water treatment plant (WTP). Columns containing Calgon F400 and Evoqua 1230AWC were fed treated water from the biologically activated carbon (BAC) topped filter beds. Phase II was conducted for 224 days using three GACs (Calgon F400, Norit GAC 400, and Hydrodarco 4000) with all influent water supplied from effluent of the BAC filtration process (Jan–Aug 2018).

Capturing Fouling with Surface Diffusion Coefficient

Data presented in SI represents an alternative fitting approach in which K was measured or estimated from pilot data directly and surface diffusion was adjusted to improve fit (all other parameters were correlated as described above). The value for 1/n was assumed to be 0.45 for all runs. This method assumes that fouling effects are captured by d_s. Calculating K directly is more straightforward than the method described above; however, these results may have limited use as concentrations, water type, or other factors are changed from the pilot conditions.

Table S1: Best fit parameter estimates for organic free Freundlich K [(μg/g)(L/μg)$^{1/n}$] and d_s [cm s^{-2}] where 1/n=0.45

Phase	Phase I Raw Inlet Water				Phase I Post-Biological Filtration				Phase II Post-Biological Filtration					
Compound	C1 Calgon F400		C2 Calgon F300		C3 Calgon F400		C4 Evoqua 1230AWC		C5 Calgon F400		C6 Hydrodarco4000		C7 Norit GAC400	
	K	d_s	K	d_s	K	d_s	K	d_s	K	d_s	K	d_s	K	d_s
PFBA	-	-	-	-	-	-	-	-	1.31	6.87E-11	0.52	1.38E-12	1.04	3.53E-13
PFPeA	-	-	-	-	-	-	-	-	2.35	2.97E-13	1.31	6.33E-13	1.97	8.10E-13
PFHxA	2.52	2.36E-13	1.92	8.18E-11	1.48	1.85E-13	1.37	2.77E-13	3.09	1.56E-13	2.45	4.38E-13	2.33	3.34E-13
PFHpA	2.09	1.33E-13	1.94	2.84E-13	1.65	1.62E-13	1.52	1.94E-13	3.08	1.40E-13	3.10	5.86E-13	2.82	1.47E-13
PFOA	2.28	8.09E-14	1.96	1.18E-13	1.98	3.16E-13	1.83	1.12E-13	2.49	8.55E-14	2.96	1.35E-13	2.57	1.01E-13
PFNA	1.34	5.80E-14	1.16	8.86E-12	1.55	6.54E-14	1.46	6.77E-14	2.70[m]	2.94E-10	2.82	2.37E-11	2.27	2.01E-11
PFDA	1.20	4.72E-11	0.97	6.52E-11	1.74	5.99E-14	1.73	7.87E-14	1.90[m]	3.50E-10	2.28	2.44E-11	1.78[↓]	4.80E-14
PFBS	1.40	2.03E-13	1.14	2.78E-10	1.15	2.74E-13	0.90	1.82E-13	1.95	7.12E-10	1.50	2.61E-10	1.38	1.09E-09
PFHxS	1.95	1.02E-10	1.89	2.49E-12	1.76	1.24E-13	1.72	1.04E-13	2.23	1.81E-10	3.11	8.63E-11	2.47	1.48E-13
PFOS	4.07	8.38E-14	3.55	3.19E-11	4.15	1.34E-13	4.27	1.34E-10	4.28	4.70E-14	7.74	2.18E-10	7.66	2.39E-14
PFMOAA*	-	-	-	-	-	-	-	-	20.9	2.77E-13	13.7	1.42E-12	15.5	6.06E-13
PFO2HxA*	-	-	-	-	-	-	-	-	5.73	1.35E-13	7.34	1.66E-13	4.20	2.97E-13
PFO3OA*	-	-	-	-	-	-	-	-	4.85	1.08E-13	10.3	4.81E-14	6.04	1.77E-13
GenX	2.31	1.74E-13	1.87	3.39E-13	1.89	2.41E-13	1.69	2.96E-13	1.91	3.08E-13	1.35	5.15E-13	2.07	4.34E-13
PFO4DA*	-	-	-	-	-	-	-	-	8.45	2.81E-14	26.0	9.14E-15	8.48	2.27E-14
Nafion BP2*	-	-	-	-	-	-	-	-	4.31	5.14E-14	5.58	6.66E-14	4.51	5.96E-14

*indicates estimated analytical values for compounds

[m]no breakthrough occurred during pilot study, capacity is expected to be greater than value calculated from data

[↓]limited breakthrough data

-no data for these compounds collected during Phase I to perform capacity calculation

Table S2: Predicted bed regeneration interval in days—Configuration of eight beds with two beds per cycle

	19 MGD			44 MGD		
Type of GAC	Average Conc.	75% of Ave. Conc.	200% of Ave Conc.	Average Conc.	75% of Ave. Conc.	200% of Ave Conc.
C1-Calgon F400	281	887	93	119	420	38
C2-Calgon F300	254	821	83	109	392	34
C3-Calgon F400	235	906	77	102	429	32
C4-Evoqua 1230AWC	183	754	58	81	343	24
C5-Calgon F400	279	1269	96	123	550	41
C6-Hydrodarco4000	293	1152	72	123	523	30
C7-Norit GAC400	336	1486	83	141	702	37

Summary:

The majority of D_s values were determined to be reduced by 10^{-4}, which was the limit of the search range. Of these, many of the resulting SSQ plots showed that little improvement of fit occurred past a reduction of ~10^{-2}, but the minimum of the analysis was used. This showed that fit was somewhat insensitive to D_s, but also was impacted by the limited number of samples to which the model was fit.

Table S3: Comparison of Predicted Bed Replacement Intervals with Uncertainty for Each Approach

	19 MGD (K & 1/n fit)			19 MGD (D_s Fit)		
Type of GAC	-10% K +10% 1/n	Best Fit K&1/n	+10% K -10% 1/n	-10%	Best Fit D_s	+10%
C1-Calgon F400 (Phase I)	187	260	357	214	281	366
C3-Calgon F400 (Phase I)	166	231	334	178	235	307
C5-Calgon F400 (Phase II)	278	423	620	203	279	385

Figure S1a – Performance model output from PSDM tool for all PFAS/GAC combinations – C1-Calgon F400

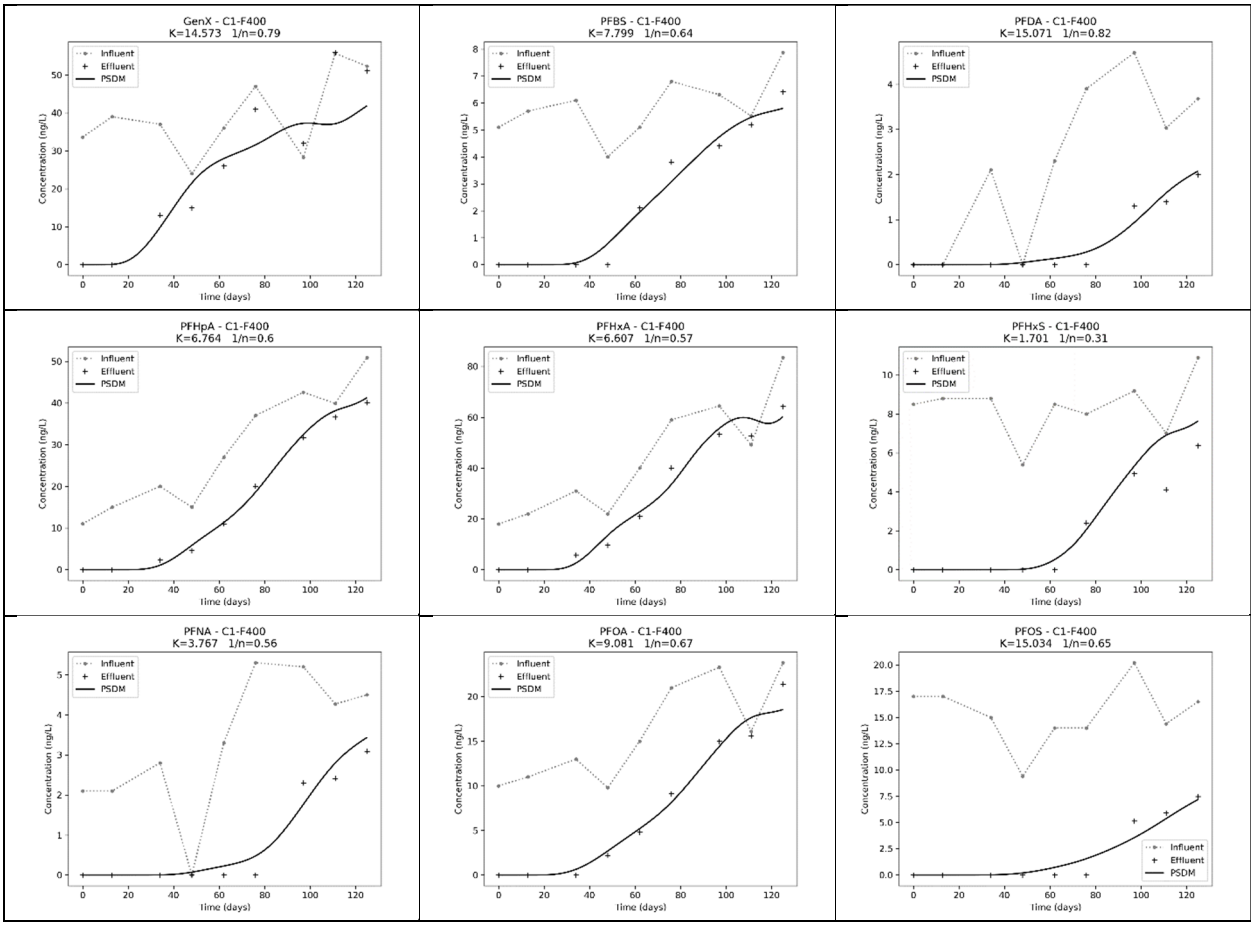

Figure S1b – Performance model output from PSDM tool for all PFAS/GAC combinations – C2-Calgon F300

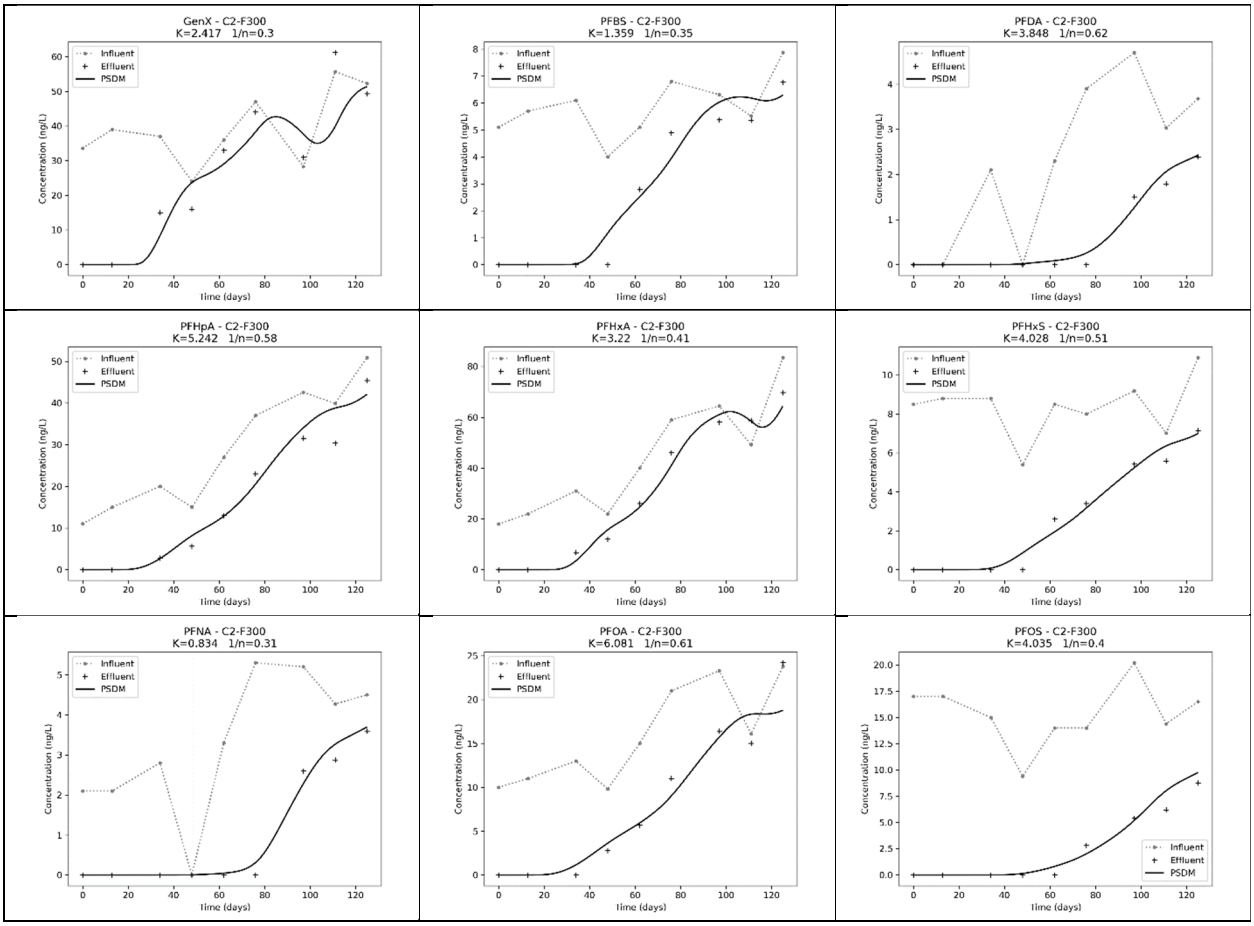

Figure S1c – Performance model output from PSDM tool for all PFAS/GAC combinations – C3-Calgon F400

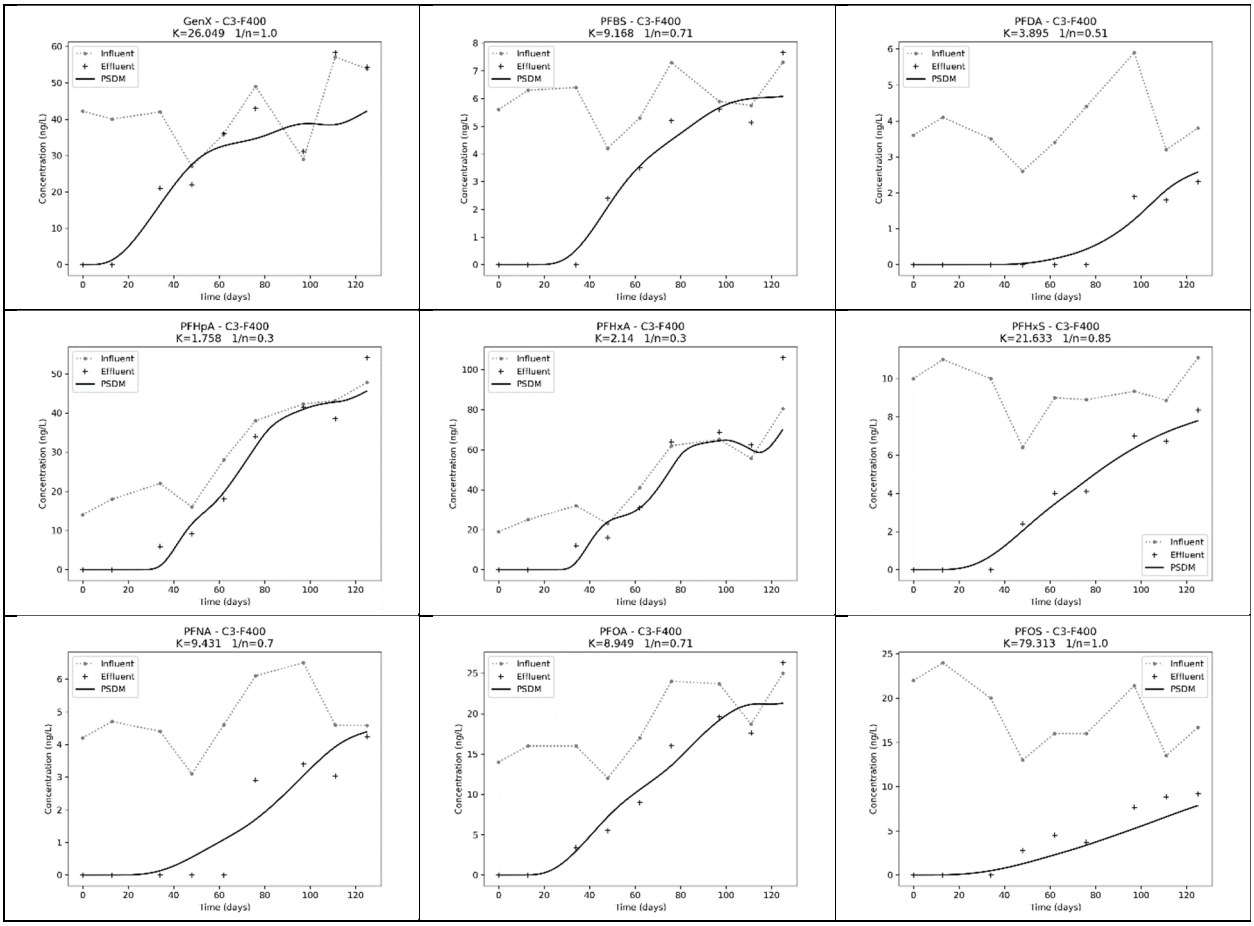

Figure S1d – Performance model output from PSDM tool for all PFAS/GAC combinations – C4-Evoqua 1230AWC

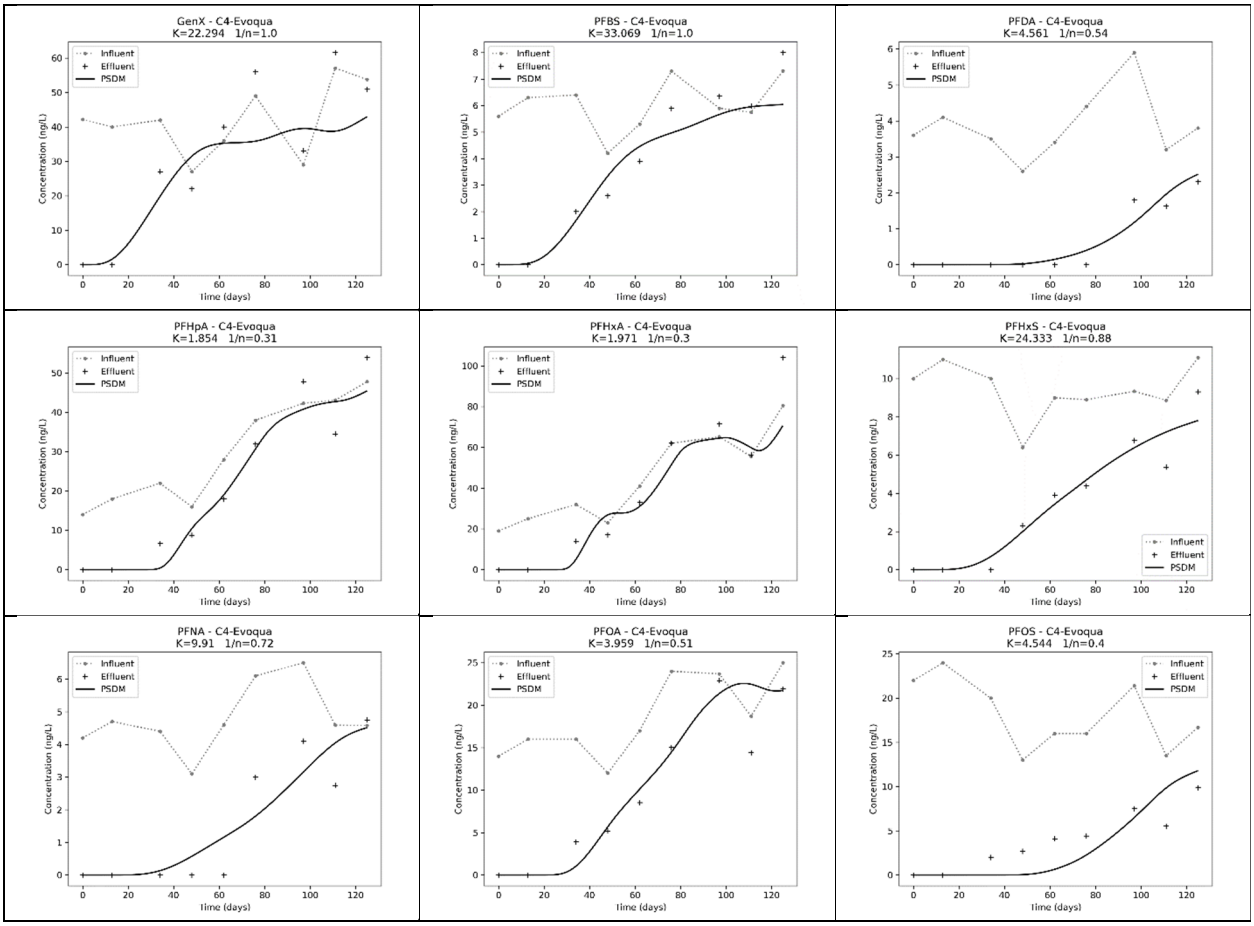

Figure S1e – Performance model output from PSDM tool for all PFAS/GAC combinations – C5-Calgon F400 (Images reflect pilot column numbering C5=C10, change made to simplify article)

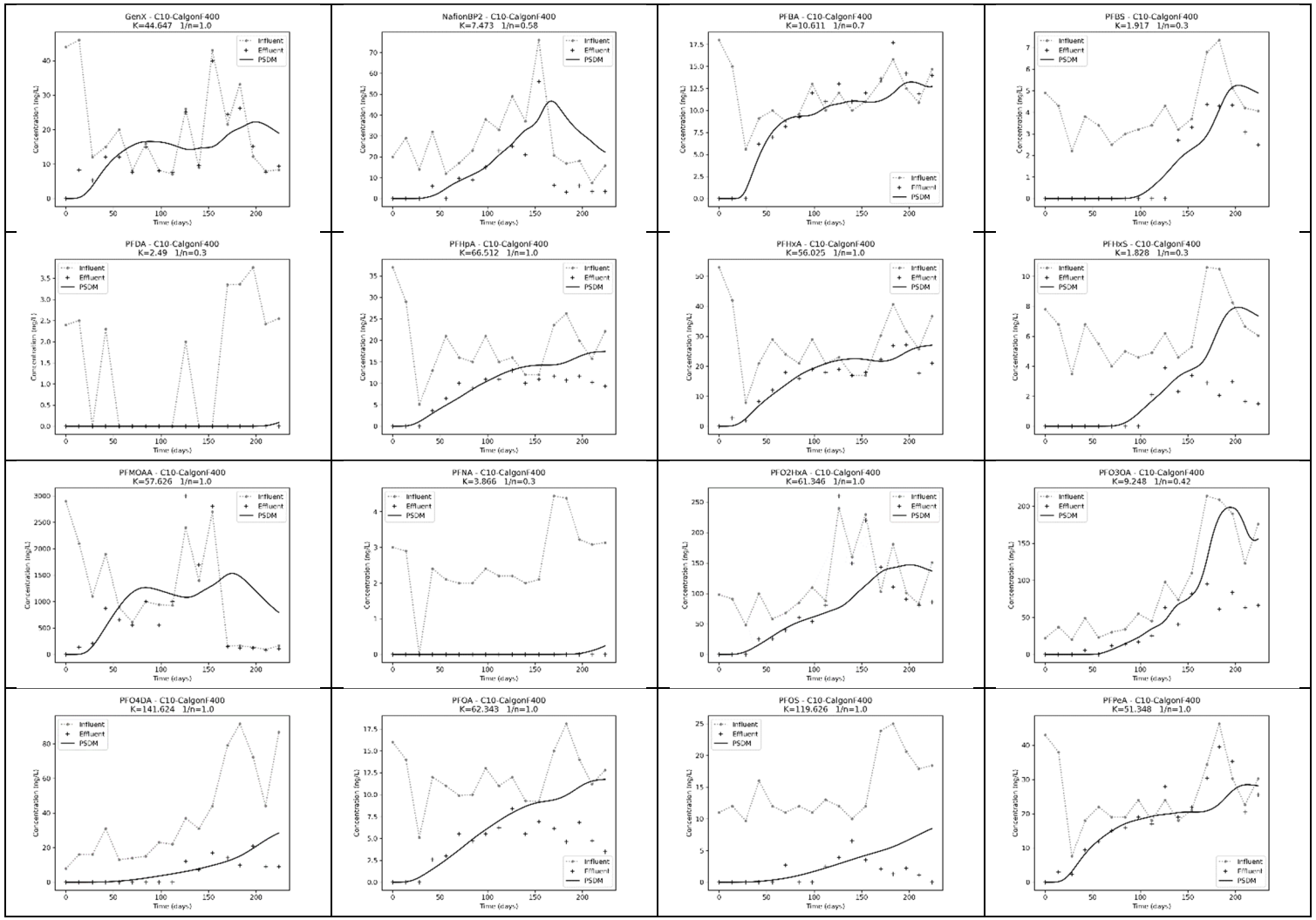

Figure S1f – Performance model output from PSDM tool for all PFAS/GAC combinations – C6-Hydrodarco4000 (Images reflect pilot column numbering C6=C12, change made to simplify article)

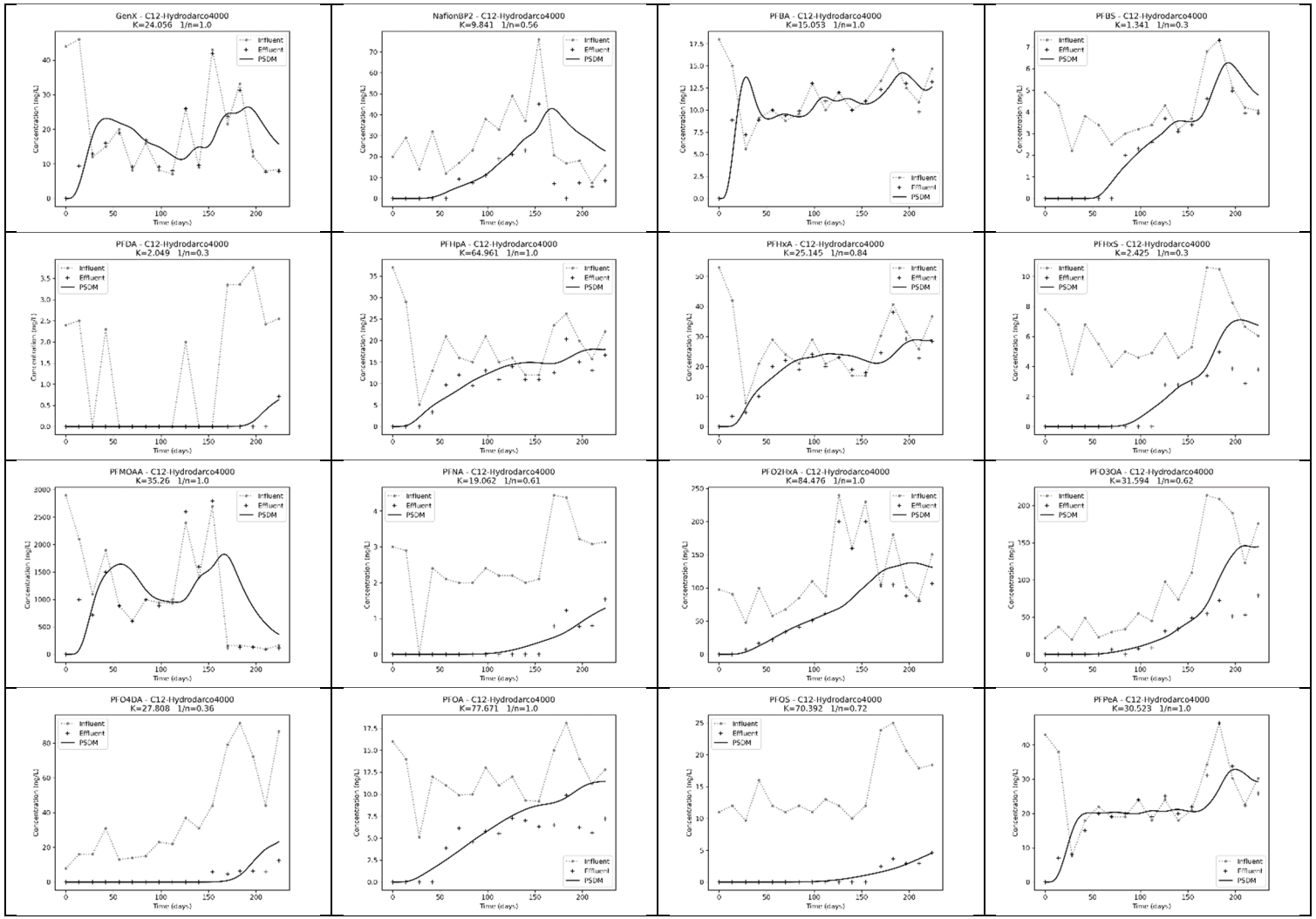

Figure S1g – Performance model output from PSDM tool for all PFAS/GAC combinations – C7-Norit GAC400 (Images reflect original pilot column numbering C7=C13, change made to simplify article)

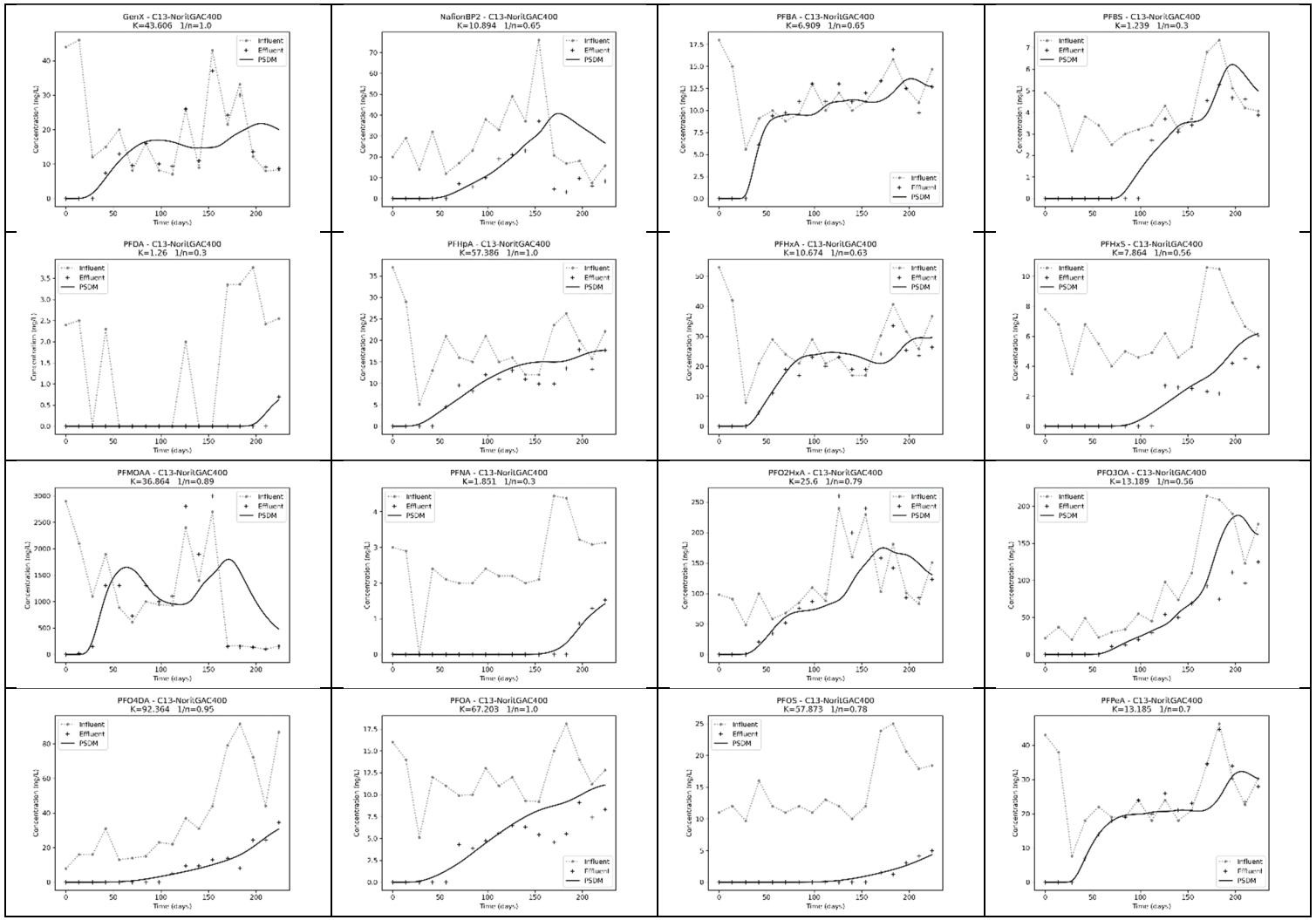

Figure S2. Nomograph indicating predicted bed replacement intervals

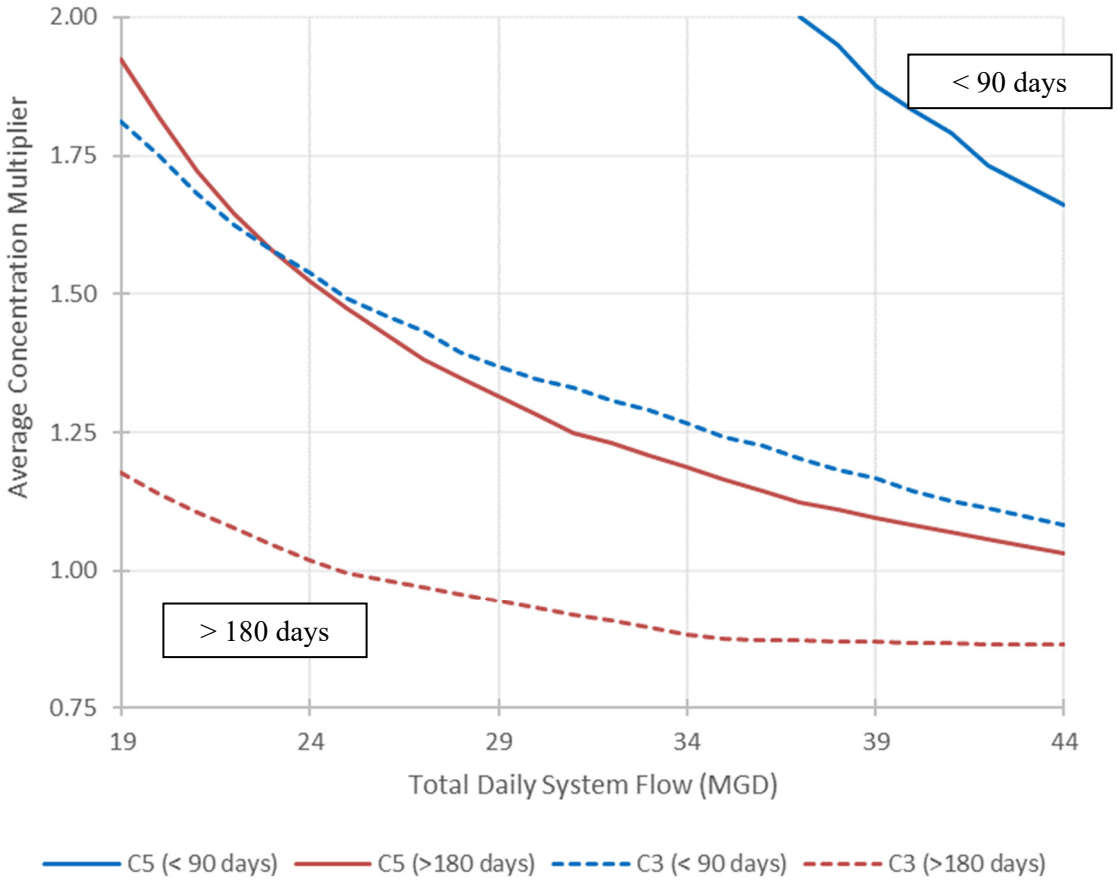

Figure S2 graphically depicts the projected bed replacement interval regions for both GACs C3 and C5—the GAC that was tested on similar water in both phases of the pilot. The region to the left or below each line corresponds to a bed replacement interval that exceeds the value for the line—where the lower left corner would have predicted bed replacement intervals that exceed 180 days. Regions that are between the same types of lines—dotted or solid—indicate a region where bed replacement is between 90 and 180 days, and the remaining upper region would be expected to require bed replacements more frequently than 90 days. This type of visualization can help systems understand how changes in either average concentrations to the system or system production capacity impact the required bed replacement intervals.

Figure S3: Comparison of Calgon F400 parameters wen considering +/- 10% K & 1/n uncertainty for Phases I (C3) and II (C5). (Darker shade = +/-10% of K, lighter shade = +/-10%K and 1/n)*

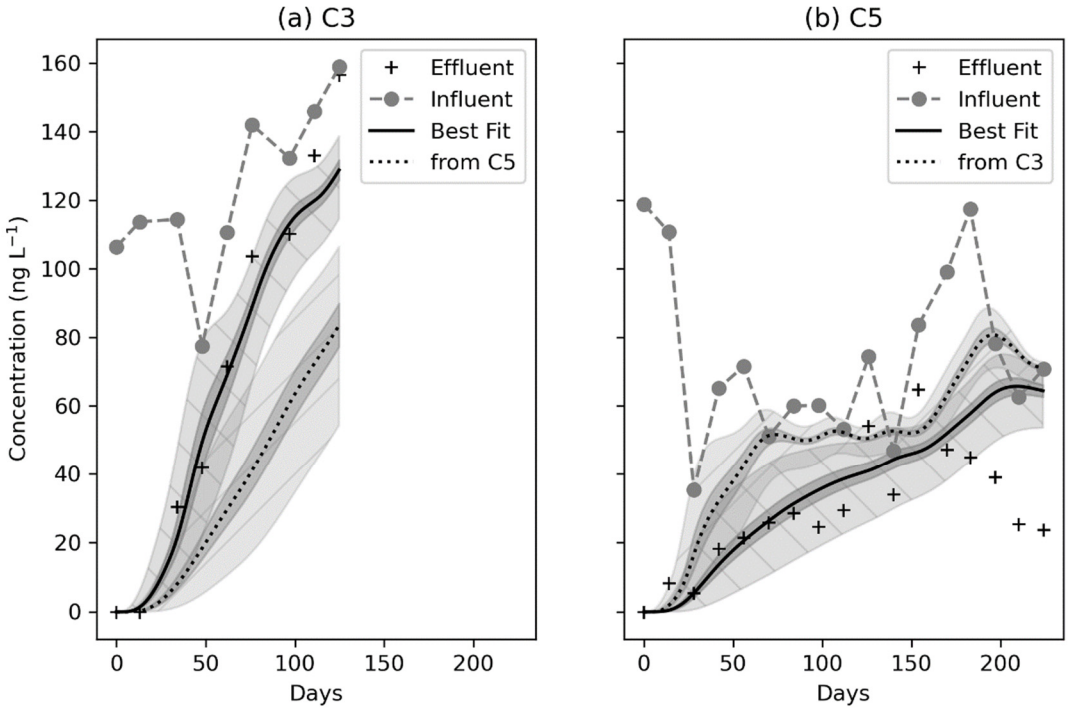

*Figure S3 plot shows shaded uncertainty regions, which are the sum of each individual PFAS uncertainty (i.e., the concentration bounds through time are the sum of the each PFAS at +10%K, -10%K, [+10%K & -10%1/n] or [-10%K & +10%1/n]). Note the opposing signs for K&1/n, because increasing K and reducing 1/n serve to increase capacity (or vis-a-versa).

Figure S4: Example of Bed Replacement Interval Projections for Calgon F400 (data from Column 1 in Table 2) [Legend key = MGD-#×mean influent concentration]

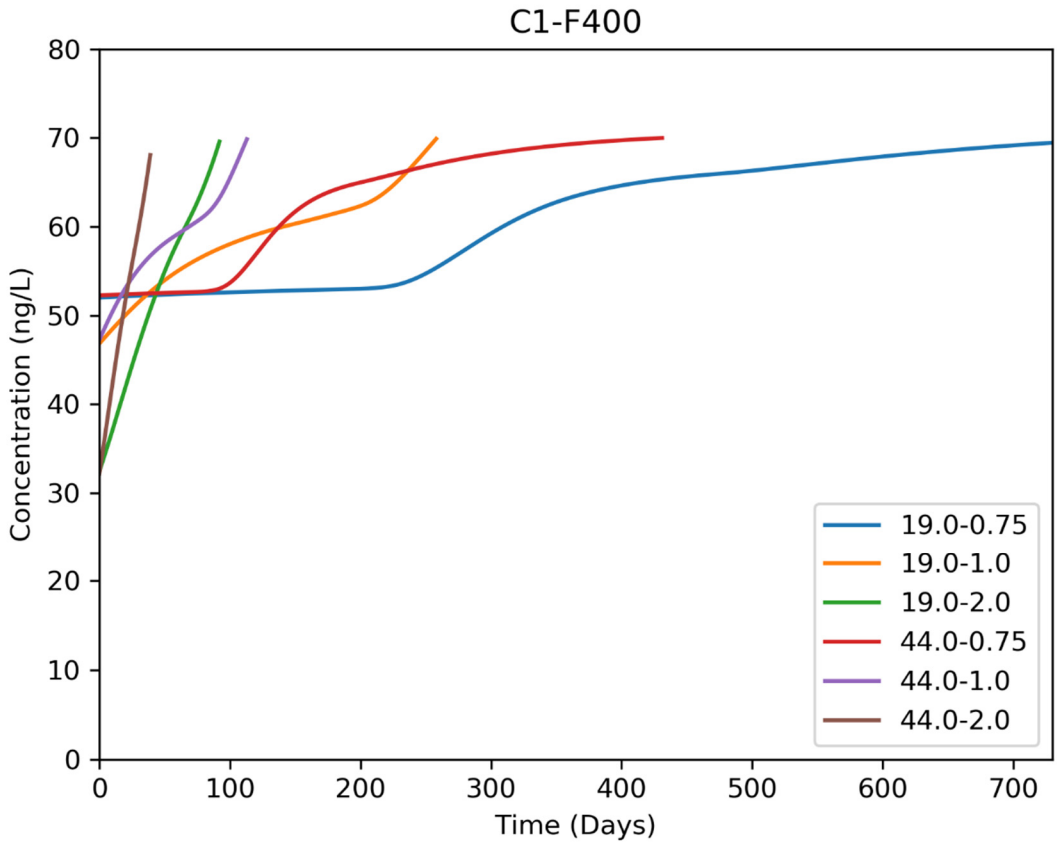

Figure S5: Expected Totalized Effluent Concentration for 6 PFAS for each GAC at 19 MGD Flow for Average Influent Concentration

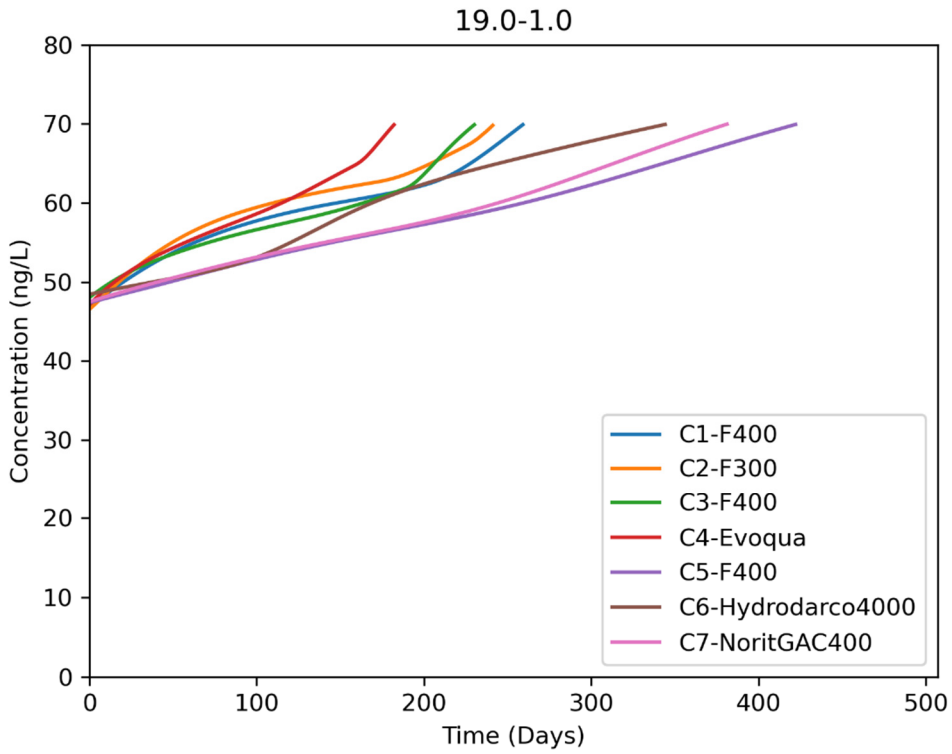

Figure S6: Comparison to linearized assumption of 1/n=1.

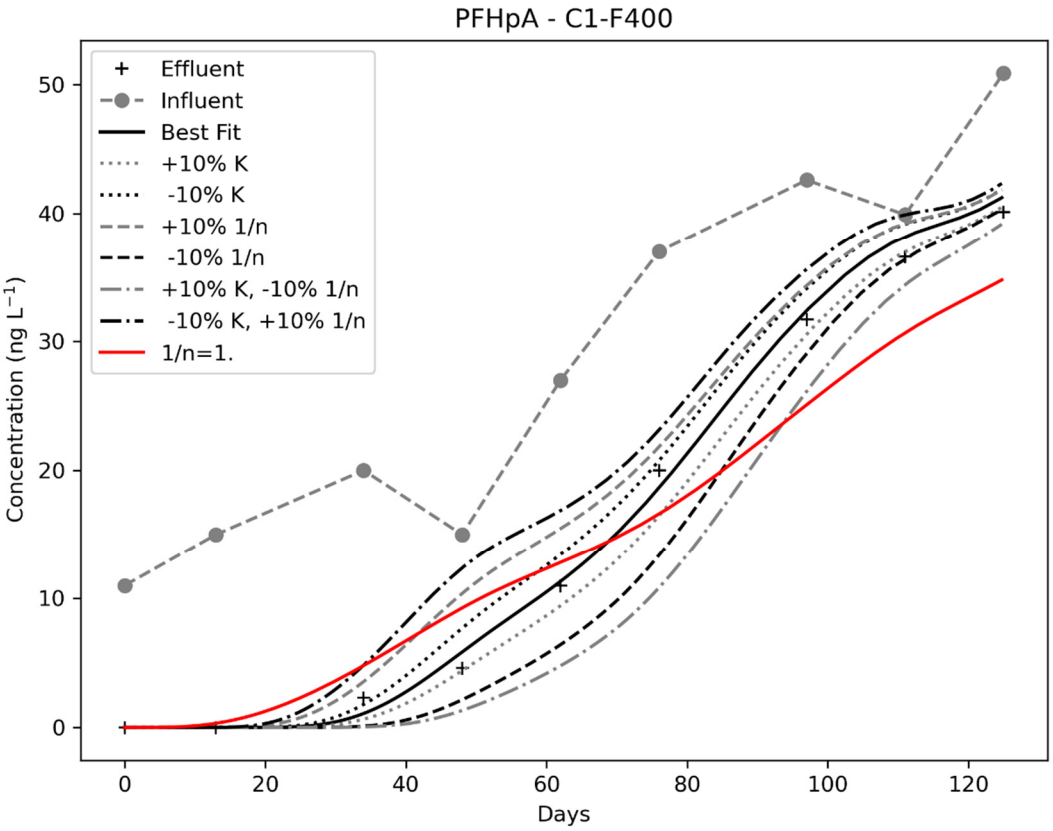

The 1/n=1 line in Figure S6 was generated by restricting the best-fit capacity search space to only consider 1/n=1. This was done to compare to the K* method used by Corwin and Summers (2011). As can be seen the 1/n=1 line does not fit the experimental data well. This is likely because the timeframe over which adsorption is occuring in this pilot was too short for the NOM to have the linearizing effect that was observed by Corwin and Summers. Table 2 does show that some of the compounds had best-fit 1/n's that were 1, or near 1. By allowing 1/n to explore a range of values, the model can ensure that initial breakthrough periods are captured well. Having reasonable estimates for that initial breakthrough may be critical for addressing complex treatment objectives that may contain summed or individual concentrations that could have low concentrations. Considering Figure S6, the concentration for the linearized model at 20 days is not reached in the best-fit case until almost day 40, which could make GAC seem less effective than it could be for a given site if that corresponded to the treatment objective.

Estimation of QSPR Correlation Factors for Capacity Reduction Equation

The PSDM model directly accounts for changes in GAC capacity over time due to natural organic matter (NOM) preloading. This relationship has been represented as the time dependent Freundlich K (K_t) divided by the Freundlich K in organic-free water (K_o). Bhuvendralingam developed a correlation that related the capacity reduction for a given contaminant to that for trichloroethene [1].

$$(K_t / K_o)_{contaminant} = a\,(K_t / K_o)_{TCE} + b \quad \text{(Eqn S1)}$$

where a and b are the correlating factors. For specific compounds, the values of a and b can be estimated using the quantitative structure property relationships [2]:

$$a = -0.0624 \log K_{ow} - 1.15 \log \kappa_2 - 0.166\, N_{am} + 1.37 \quad \text{(Eqn S2)}$$

$$b = 0.0441\, \alpha + 0.406\, D_{z(hybrid)} - 0.250 \quad \text{(Eqn S3)}$$

where K_{ow} is the octanol-water partition coefficient, κ_2 is the second-order shape index, N_{am} is the sum of the number of primary and secondary amine groups, α is the molecular polarizability calculated by Dgauss (DZYP basis set), and $D_{z(hydrbid)}$ is the largest hybrid component of the dipole moment perpendicular to the long molecular axis. $D_{z(hydrbid)}$ was calculated with MOPAC 2000 (PM3 basis set) and was manually extracted from the MOPAC 2000 output file. For all chemicals in Table S1, N_{am} is 0. The other parameters were calculated as described in [2].

Table S4: Values used to calculate QSPR a & b parameters.

Compound (acronym)	CAS#	*log* K_{ow}	*log* K_{ow} error	κ_2	N_{am}	α	$D_{z(hybrid)}$	QSPR Fouling Parameters	
								a	b
Perfluorobutanoic acid (PFBA)	375-22-4	-0.66[a]	0.08	3.29	0	8.36	0.001	0.82	0.12
Perfluoropentanoic acid (PFPeA)	2706-90-3	0.03[a]	0.08	4.03	0	10.05	0.001	0.67	0.19
Perfluorohexanoic acid (PFHxA)	307-24-4	0.69[a]	0.10	4.78	0	11.93	0.001	0.55	0.28
Perfluoroheptanoic acid (PFHpA)	375-85-9	1.30[a]	0.08	5.52	0	13.83	0.001	0.44	0.36
Perfluorooctanoic acid (PFOA)	335-67-1	1.89[a]	0.10	6.27	0	15.74	0.001	0.34	0.44
Perfluorononanoic acid (PFNA)	375-95-1	2.57[a]	0.07	7.02	0	17.66	0	0.24	0.53
Perfluorodecanoic acid (PFDA)	335-76-2	2.90[a]	0.10	7.77	0	19.59	0	0.17	0.61
Perfluorobutanesulfonic acid (PFBS)	375-73-5	0.029	0.001	4.00	0	12.20	-0.122	0.68	0.24
Perfluorohexanesulfonic acid (PFHxS)	355-46-4	1.24	0.04	5.50	0	16.08	0.042	0.44	0.48
Perfluoroheptanesulfonic acid (PFHpS)	375-92-8	1.84	0.06	6.25	0	18.02	0.052	0.34	0.57
Perfluorooctanesulfonic acid (PFOS)	1763-23-1	2.45[a]	0.08	7.00	0	19.96	0.083	0.25	0.66
Perfluoro-2-methoxyacetic acid (PFMOAA)	674-13-5	1.32	0.04	3.16	0	6.98	-0.006	0.88	0.055
Perfluoro(3,5-dioxahexanoic) acid (PFO2HxA)	39492-88-1	-0.126	-0.004	4.47	0	9.45	-0.001	0.63	0.17
Perfluoro(3,5,7-trioxaoctanoic) acid (PFO3OA)	39492-89-2	1.06	0.03	5.78	0	11.94	-0.023	0.43	0.27
Perfluoro-2-proxypropanoic acid (PFPrOPrA/GenX)	13252-13-6	0.54	0.02	5.33	0	12.58	0.08	0.50	0.37
Perfluoro(3,5,7,9-tetraoxadecanoic) acid (PFO4DA)	39492-90-5	2.25	0.07	7.09	0	14.45	-0.054	0.25	0.37
Ethanesulfonic acid, 2-1[1-[difluoro(1,2,2,2-tetrafluoroethoxy)methyl]-1,2,2,2-tetrafluoroethoxy]-1,1,2,2-tetrafluoro-(Nafion BP2)	749836-20-2	1.41	0.05	7.36	0	18.82	0.123	0.29	0.63
6:2 Fluorotelomer sulfonic acid (62FTS)	27619-97-2	0.84	0.03	6.56	0	18.98	0.088	0.38	0.62
8:2 Fluorotelomer sulfonic acid (82FTS)	39108-34-4	2.05	0.07	8.05	0	22.85	0.087	0.20	0.79

[a] Experimental data by Jing [3]

There are few experimental data for K_{ow} for PFASs since they tend accumulate at the interface between octanol and water, eliminating traditional approaches for measuring K_{ow}. The limited experimental data indicated in Table S4 were all obtained by Jing using ion transfer cyclic voltammetry [3], with the K_{ow} values and errors calculated from the thermodynamic parameters as listed in Jing's supporting information. These are also the values used by Hidalgo [4] in estimating K_{ow} values for which Jing did not report data. Rayne also included Jing's values in their review of perfluoroalkyl sulfonic acid (PFSA) and perfluoroalkyl carboxylic acids (PFCA) physiochemical properties [5]. Ding [6] and Kim [7] list slightly different values in their studies, especially for PFBA and PFPA.

Because experimental data is not available for the majority of compounds, Table S4 presents estimates of log K_{ow} via an approach that builds on Hidalgo's observation that the slopes of the linear regression of PFCA or PFSA log K_{ow} values versus carbon change length are expected to be essentially the same [4]. Hidalgo predicted values for PFSAs based on the value for PFOS reported by Jing [3] and the experimental slope for the PFCAs. Analogous to this approach, the estimates for PFSAs are based on the slope of the plot shown in Figure S7, which is the Jing's PFCAs values for K_{ow} versus EPA EPISUITE's estimation of log K_{ow} via its KOWWIN module [8]. r^2 is 0.9948 with the p value at the 95% confidence level of 6.7×10^{-7}, indicating that the trends are significant at the 95% confidence level.

The calculations in Figure S7 above were made with KOWWIN version 1.68, which includes a group contribution factor for -CF_2- groups. Jing [3] and Rayne [5] did not report this correlation when utilizing EPISUITE, although probably used earlier version of KOWWIN based on the dates of their publications. This type of linear extrapolation to develop estimates was also used by Kim [7], although instead of the KOWWIN output, they used molar volume as the basis of the linear relationship, they when combined with Jing's data resulting in $r^2 = 0.8989$, which might reflect an experimental value for PFBS referenced in seeming error to Jing (Kim's Supplemental Table S4).

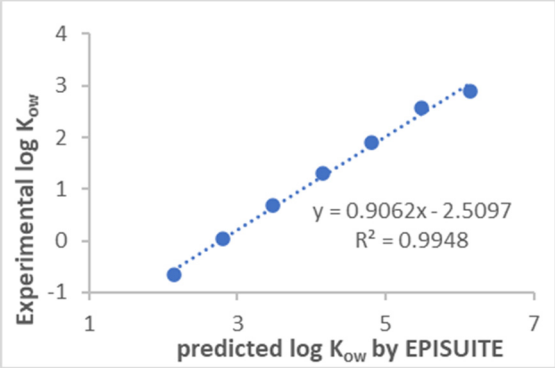

Figure S7. Correlation of experimental versus predicted log K_{ow} values. The standard errors of the slope and intercept, as calculated by Microsoft Excel regression analysis, are 0.03 and 0.1, respectively.

While there are no experimental data to verify the estimations of PFBS, PFHxS, and PFHptX, it is reassuring to note that Hildago, building on Jing and others, observed "the structural differences of the head group (sulfonate or carboxylate) do not produce Log P (K_{ow}) differences between PFSs and PFCs, as long as they have the same number of carbon atoms in the perfluorinated alkyl chain. That is, the Log P (K_{ow}) of the PFS with N carbon atoms should be very similar to the Log P (K_{ow}) value of the PFC with N + 1 carbon atoms. Indeed, the values of PFBS, PFHxS, and PFHptX are the same (within experimental error) of PFPeA, PFHptA, and PFOA, just like PFOS's experimental value is similar to PFNA's.

In Table S4, among compounds that are not PFCAs or PFSAs, for those that contain carboxylate head groups, log K_{ow} is estimated via the linear relationship in Figure S7. For the remaining compounds in Table S4 that contain sulfonate groups, log K_{ow} is estimated via the same equation used for the PFSAs. These compounds are not linear change homologues, so the direct applicability of this approach can not be verified without experimental data. However, KOWWIN 1.68 contains a factor for the ether linkage (-OCF2-), perhaps reassuring considering that the factor used in KOWWIN1.68 for -CF2- resulted in Figure S7.

Until further data is available to verify these compounds, the log K_{ow}'s can be viewed as transparently and systematically predicted. Note that ether linkages affect the geometry of the respective molecules, and those geometry changes are accounted for in the other descriptors in Table S4 and, hence, the calculated a and b values (Eqns S2 and S3). From a practical standpoint, it is interesting to perform a sensitivity analysis of the effect of log K_{ow} uncertainty on the capacity reduction (Eqn S1).

Assuming a 0.5 fold (50%) reduction in $(K_t/K_0)_{TCE}$, it is evident in Table S2 that only when K_{ow} changes by large values (2–3), does the impact of K_{ow} uncertainty upon capacity reduction become greater than 10%. Thus, extremely accurate determination and/or prediction of log K_{ow} is likely not necessary to practically apply these capacity reduction equations.

Table S5. Sensitivity analysis for capacity reduction for several uncertainties in the K_{ow} values presented in Table S4.

		Capacity reduction for K_{ow} uncertainties						
Compound (acronym)	**CAS#**	K_{ow} -3	K_{ow} -2	K_{ow} -1	K_{ow}	K_{ow} +1	K_{ow} +2	K_{ow} +3
Perfluorobutanoic acid (PFBA)	375-22-4	0.62	0.59	0.56	0.53	0.50	0.46	0.43
Perfluoropentanoic acid (PFPeA)	2706-90-3	0.62	0.59	0.56	0.53	0.50	0.47	0.44
Perfluorohexanoic acid (PFHxA)	307-24-4	0.64	0.61	0.58	0.55	0.52	0.49	0.46
Perfluoroheptanoic acid (PFHpA)	375-85-9	0.67	0.64	0.61	0.58	0.55	0.52	0.49
Perfluorooctanoic acid (PFOA)	335-67-1	0.71	0.67	0.64	0.61	0.58	0.55	0.52
Perfluorononanoic acid (PFNA)	375-95-1	0.74	0.71	0.68	0.65	0.62	0.59	0.55
Perfluorodecanoic acid (PFDA)	335-76-2	0.79	0.76	0.73	0.70	0.67	0.64	0.60
Perfluorobutanesulfonic acid (PFBS)	375-73-5	0.67	0.64	0.61	0.58	0.55	0.51	0.48
Perfluorohexanesulfonic acid (PFHxS)	355-46-4	0.79	0.76	0.73	0.70	0.67	0.63	0.60
Perfluoroheptanesulfonic acid (PFHpS)	375-92-8	0.83	0.80	0.77	0.74	0.71	0.67	0.64
Perfluorooctanesulfonic acid (PFOS)	1763-23-1	0.88	0.85	0.82	0.79	0.76	0.73	0.69
Perfluoro-2-methoxyacetic acid (PFMOAA)	674-13-5	0.59	0.56	0.52	0.49	0.46	0.43	0.40
Perfluoro(3,5-dioxahexanoic) acid (PFO2HxA)	39492-88-1	0.57	0.54	0.51	0.48	0.45	0.42	0.39
Perfluoro(3,5,7-trioxaoctanoic) acid (PFO3OA)	39492-89-2	0.57	0.54	0.51	0.48	0.45	0.42	0.39
Perfluoro(3,5,7,9-tetraoxadecanoic) acid (PFO4DA)	39492-90-5	0.58	0.55	0.52	0.49	0.46	0.43	0.40
Perfluoro-2-proxypropanoic acid (PFPrOPrA/GenX)	13252-13-6	0.68	0.65	0.62	0.59	0.56	0.53	0.49
Ethanesulfonic acid, 2-1[1-[difluoro(1,2,2,2-tetrafluoroethoxy)methyl]-1,2,2,2-tetrafluoroethoxy]-1,1,2,2-tetrafluoro- (Nafion BP2)	749836-20-2	0.87	0.83	0.80	0.77	0.74	0.71	0.68
6:2 Fluorotelomer sulfonate (62FTS)	425670-75-3	0.91	0.87	0.84	0.81	0.78	0.75	0.72
8:2 Fluorotelomer sulfonate (82FTS)	481071-78-7	0.99	0.96	0.92	0.89	0.86	0.83	0.80

Literature Cited

[1] S. Bhuvendralingam, A decision algorithm for optimizing granular activated carbon adsorption process design, in, Michigan Technological University, 1992.

[2] M.L. Magnuson, T.F. Speth, Quantitative structure− property relationships for enhancing predictions of synthetic organic chemical removal from drinking water by granular activated carbon, Environmental science & technology, 39 (2005) 7706–7711.

[3] P. Jing, P.J. Rodgers, S. Amemiya, High lipophilicity of perfluoroalkyl carboxylate and sulfonate: Implications for their membrane permeability, Journal of the American Chemical Society, 131 (2009) 2290–2296.

[4] A. Hidalgo, N. Mora-Diez, Novel approach for predicting partition coefficients of linear perfluorinated compounds, Theoretical Chemistry Accounts, 135 (2016) 18.

[5] S. Rayne, K. Forest, Perfluoroalkyl sulfonic and carboxylic acids: A critical review of physicochemical properties, levels and patterns in waters and wastewaters, and treatment methods, Journal of Environmental Science and Health Part A, 44 (2009) 1145–1199.

[6] G. Ding, W.J. Peijnenburg, Physicochemical properties and aquatic toxicity of poly-and perfluorinated compounds, Critical reviews in environmental science and technology, 43 (2013) 598–678.

[7] M. Kim, L.Y. Li, J.R. Grace, C. Yue, Selecting reliable physicochemical properties of perfluoroalkyl and polyfluoroalkyl substances (PFASs) based on molecular descriptors, Environmental pollution, 196 (2015) 462–472.

[8] U. EPA, Exposure Assessment Tools and Models, Estimation Program Interface (EPI) Suite, V 4.11, in, US Environmental Protection Agency, Exposure Assessment Branch Washington, DC, 2012.